Identifying instrumental and historical earthquake records in the SW Iberian margin using ^{210}Pb turbidite chronology

Jordi Garcia-Orellana,[1,2] Eulàlia Gràcia,[3] Alexis Vizcaino,[3]
Pere Masqué,[1,2] Carolina Olid,[1] Francisca Martínez-Ruiz,[4]
Elena Piñero,[3] Joan-Albert Sanchez-Cabeza,[1,2,5] and Juanjo Dañobeitia[3]

Received 12 October 2006; revised 10 November 2006; accepted 14 November 2006; published 16 December 2006.

[1] Textural, mineralogical and geochemical analyses of near-surface sediments from six different stations offshore SW Iberian Peninsula revealed the presence of thin detrital intervals corresponding to very fine-grained turbidites. Precise dating of the two most recent sedimentary layers based on ^{210}Pb and ^{137}Cs geochronology provides ages of 1971 ± 3 AD and 1908 ± 8 AD. These ages correspond to high-magnitude historical and instrumental earthquakes that occurred in the region: the 1969 Horseshoe Earthquake (Mw 8.0) and the 1909 Benavente Earthquake (Mw 6.0). Such a good correlation between turbidites and high-magnitude (Mw > 6) historical and instrumental seismic events suggests that the record of mass transport deposits can also be used as a paleoseismic indicator in low-convergence margins. **Citation:** Garcia-Orellana, J., E. Gràcia, A. Vizcaino, P. Masqué, C. Olid, F. Martínez-Ruiz, E. Piñero, J. A. Sanchez-Cabeza, and J. Dañobeitia (2006), Identifying instrumental and historical earthquake records in the SW Iberian margin using ^{210}Pb turbidite chronology, *Geophys. Res. Lett.*, *33*, L24601, doi:10.1029/2006GL028417.

1. Introduction

[2] Crustal deformation in the southwestern margin of the Iberian Peninsula is controlled by the NW-SE convergence of the African and Eurasian Plates (4.5–5.6 mm·yr^{-1}) at the eastern end of the Azores-Gibraltar zone [*Argus et al.*, 1989; *DeMets et al.*, 1990]. This convergence is accommodated through a wide deformation zone [e.g., *Grimison and Chen*, 1986; *Sartori et al.*, 1994]. The SW Iberian Margin is characterized by moderate-magnitude seismicity [e.g., *Buforn et al.*, 1995, 2004; *Stich et al.*, 2005a], although great earthquakes (Mw > 8) such as the 1755 Lisbon Earthquake and the 1969 Horseshoe Earthquake [e.g., *López Arroyo and Udías*, 1972; *Fukao*, 1973; *Mezcua et al.*, 2004] have also occurred in this region (Figure 1). Recently acquired marine geophysical data revealed a number of active west-verging thrusts (e.g., Marques de Pombal, Sao Vicente, and Horseshoe faults) located <100 km offshore Portugal [*Zitellini et al.*, 2001; *Gràcia et al.*, 2003a, 2003b; *Terrinha et al.*, 2003] (Figure 1). The recognition of deformed Quaternary units together with swarms of superficial seismicity associated with the ruptures [*Gràcia et al.*, 2003a; *Buforn et al.*, 2004; *Stich et al.*, 2005a] suggests that thrusts located beneath these ruptures are active, and that they may increase the seismic and tsunami hazard along the coasts of the Iberian Peninsula and North Africa. Associated with active faulting, submarine landslides and resulting mass transport deposits (debris flows and turbidites) have also been recognized in the Marques de Pombal Fault area, providing information of the Holocene earthquake record [e.g., *Vizcaino et al.*, 2006]. In order to investigate modern sedimentation (<150 years) associated with recent seismic events in the SW Portuguese Margin, six sediment cores were collected by multicorer in the area stretching from the Tagus to the Horseshoe Abyssal Plains for radiometric (^{210}Pb and ^{137}Cs) and sedimentological analyses (Figure 1).

[3] ^{210}Pb ($T_{1/2}$ = 22.3 yr) is a widely-used radiotracer in the study of sedimentary environments on a temporal scale of 100–150 years [e.g., *Robbins and Edgington*, 1975; *Nittrouer et al.*, 1970; *Masqué et al.*, 2003]. This naturally-occurring radionuclide is present in sediments after formation by decay of ^{222}Rn ($T_{1/2}$ = 3.8 d) in the atmosphere and the water column ($^{210}Pb_{excess}$) and in situ decay of ^{226}Ra ($T_{1/2}$ = 1600 yr). Age models based on ^{210}Pb concentration profiles in sediment cores can be confirmed by independent time-stratigraphic markers, such as artificial radionuclides (e.g., ^{137}Cs), which allows us to discriminate the influence of postdepositional processes such as mixing. The onset of ^{137}Cs presence in sediments corresponds to the beginning of the atmospheric nuclear tests in the 1950s, and the highest concentrations correspond to maximum atmospheric activities due to nuclear tests (1963) and the Chernobyl accident (1986).

[4] A non-disturbed sediment profile would be characterised by a nearly exponential decrease in ^{210}Pb concentration with depth. In seismic studies, where turbidity flows could transport allocthonous sediment from the continental slope, irregularities are commonly observed in the ^{210}Pb concentration profiles. In such instances, accumulation rates can be derived by applying the Constant Flux Constant Sedimentation model (CF:CS) [*Krishnaswami et al.*, 1971] to the depth intervals where the ^{210}Pb concentration profile follows an exponential shape with depth [e.g., *Arnaud et al.*, 2002; *Huh et al.*, 2004, 2006].

[1]Departament de Física, Universitat Autònoma de Barcelona, Bellaterra, Spain.
[2]Institut de Ciència i Tecnologia Ambientals, Universitat Autònoma de Barcelona, Bellaterra, Spain.
[3]Unitat de Tecnologia Marina, Consejo Superior de Investigaciones Científicas, Centre Mediterrani d'Investigacions Marines i Ambientals, Barcelona, Spain.
[4]Instituto Andaluz de Ciencias de la Tierra, Consejo Superior de Investigaciones Científicas, Facultad de Ciencias, Universidad de Granada, Granada, Spain.
[5]Marine Environment Laboratories, International Atomic Energy Agency, Monaco, Monaco.

0094-8276/06/2006GL028417

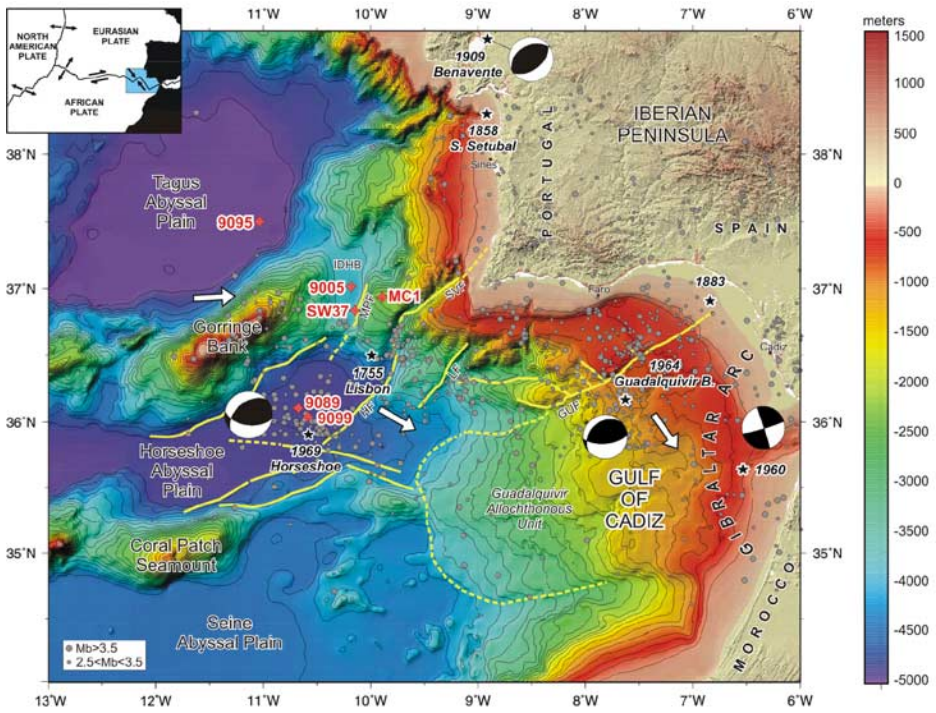

Figure 1. Plate-tectonic setting of the SW Iberian Margin, at the boundary between the Eurasian and African plates (inset) and shaded relief map of the SW Iberian Margin, based on SRTM-3 for land topography and GEBCO for bathymetry. White arrows depict plate convergence motion (4.5–5.6 mm·yr^{-1}) from the NUVEL1 model [e.g., *Argus et al.*, 1989]. Earthquake epicenters from the Spanish "Instituto Geográfico Nacional" catalog for the period between 1965 and 2003 are depicted by small grey dots (Instituto Geográfico Nacional, Catálogo sísmico nacional hasta el 2003, available at http://www.fomento.es/mfom/lang_castellano/direcciones_generales/instituto_geografico/Geofisica/sismologia/). High-magnitude historical and instrumental earthquakes that occurred in the SW Iberian Margin after the 1755 event are located, and correspond to the 1755 AD Lisbon, Mw 8.5–8.7 [*Johnston*, 1996; *Martínez-Solares and López Arroyo*, 2004]; 1858 AD Setúbal, I = IX [*Martínez-Solares*, 2003]; 1883 AD, Mw 6.1 and 1909 AD Benavente, Mw 6.6 [*Mezcua et al.*, 2004]; 1960 AD, Mw 6.2 [*Buforn et al.*, 2004]; 1964 AD Guadalquivir Bank, Mw 6.1–6.6 [*Buforn et al.*, 2004; *Stich et al.*, 2005a]; and 1969 AD Horseshoe, Mw 7.0–8.0 [*Buforn et al.*, 2004; *Stich et al.*, 2005a]. Focal mechanisms are from *Buforn et al.* [1995] and *Stich et al.* [2005a, 2005b]. Main ocean-floor elements are summarized from work by *Gràcia et al.* [2003a, 2003b] and *Zitellini et al.* [2004]. Sediment cores studied in this work are depicted.

[5] The aims of this paper are (1) to date the detrital layers identified in a high-resolution sediment core from the Marques de Pombal Fault area by using the ^{210}Pb CF:CS model constrained by ^{137}Cs chronology; (2) to correlate these ages with turbidite layers identified in other five sediment cores from neighboring abyssal plains, where lower accumulation rates prevent the use of ^{210}Pb chronology; and (3) to determine whether these regionally-correlated coeval turbidite intervals are seismically triggered and correspond to high-magnitude instrumental and historical earthquakes generated in the SW Iberian Margin.

2. Data and Methods

[6] Six sediment cores (Figure 1 and Table 1) with a maximum thickness of ~40 cm were collected using a multicore sampler with Plexiglas tubes to guarantee the preservation of the water-sediment interface, except core SW37, which was collected using a piston core trigger.

Table 1. Location of Short Sediment Cores Collected in the SW Iberian Margin[a]

Core	Cruise	Sample Collection	Location	Depth, m	Coordinates		Coring System	Accumulation Rates, cm·kyr^{-1}
					North Latitude	West Longitude		
MC1	HITS-01	10/2001	top MPF	2173	36° 56′	09° 45′	Multicorer	81 ± 7
SW37	SWIM-04	09/2004	base MPF	3895	36° 50′	10° 09′	Trigger core	55 ± 12
9005	GAP-03	12/2003	IDHB	3919	37° 01′	10° 11′	Multicorer	28 ± 4
9095	GAP-03	12/2003	TAP	5162	37° 30′	11° 02′	Multicorer	34 ± 2
9089	GAP-03	12/2003	HAP	4897	36° 06′	10° 40′	Multicorer	21 ± 1
9099	GAP-03	12/2003	HAP	4900	36° 02′	10° 35′	Multicorer	14 ± 2

[a]MPF: Marques de Pombal Fault block; IDHB: Infante Don Henrique Basin; TAP: Tagus Abyssal Plain; HAP: Horseshoe Abyssal Plain.

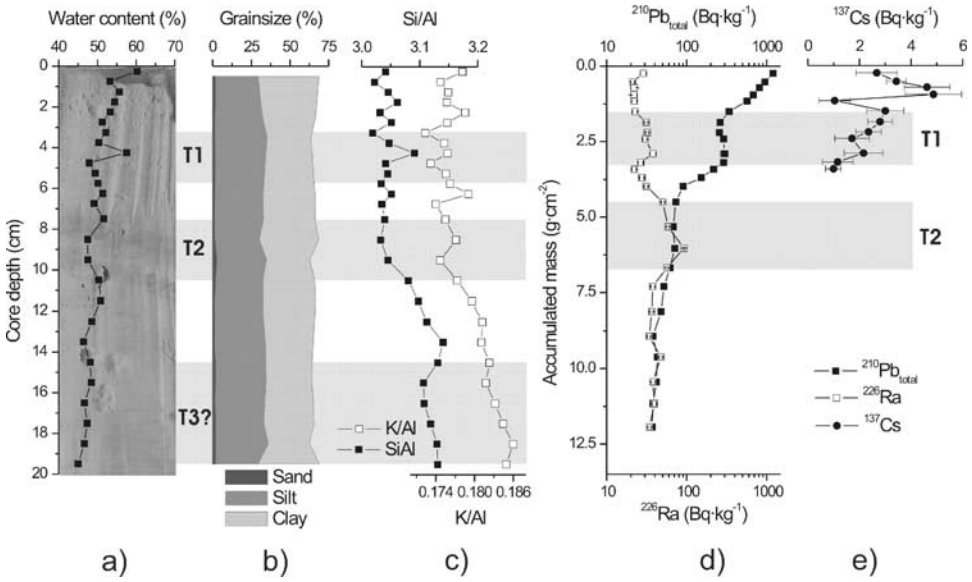

Figure 2. MC1 sediment core image, depth profiles of (a) water content, (b) grain size and (c) Si/Al – K/Al. Accumulated mass profiles of (d) $^{210}Pb_{total}$, ^{226}Ra and (e) ^{137}Cs. Grey rectangles correspond to turbidite events T1, T2 and T3.

Cores were sliced onboard into sections of 0.5 cm (from 0 to 5 cm depth), 1 cm (5 to 20 cm depth) and 2 cm (20 cm to core bottom). Grain-size analyses were performed on sediment samples from core MC1 using a settling tube for the coarse-grained (>50 μm) fraction, and a SediGraph 5100 particle size analyzer for the silt and clay (<50 μm) fractions integrated in a single textural distribution. The sand fraction and very coarse silt components (>50 μm) were identified using a binocular.

[7] Determination of ^{210}Pb activities was accomplished through the measurement of its daughter nuclide, ^{210}Po, following the methodology described by *Sanchez-Cabeza et al.* [1998]. Briefly, after addition of a given amount of ^{209}Po as internal tracer, sediment aliquots of 200–300 mg of each sample were totally dissolved in acid medium by using an analytical microwave oven. Polonium isotopes were plated onto pure silver discs and counted with α-spectrometers equipped with low-background silicon surface barrier (SSB) detectors. ^{226}Ra (via ^{214}Pb through its 351 keV emission line) and ^{137}Cs in core MC1 were determined by γ-spectrometry using a high-purity well-type Ge detector.

[8] The mineral composition of bulk and coarse fractions (>50 μm) was determined by X-ray diffraction (Philips PW 1710 diffractometer) and scans were run from 2–64° 2θ. Peak areas were measured in order to estimate semi-quantitative mineral contents. Major elements were identified using a Philips PW 2400 sequential wavelength dispersive X-ray spectrometer following standard XRF methodology.

3. Results and Discussion

[9] Deep-sea channels and abyssal plains in seismically-active areas are ideal environments for the study of turbidite paleoseismology: the use of marine turbidite record as a proxy for earthquake recurrence, which has been successfully applied in several active margins [e.g., *Adams*, 1990; *Huh et al.*, 2004; *Goldfinger et al.*, 2003, 2006]. However, the determination of an age model of modern events (<150 yr) in these deep marine environments can be challenging, mainly because accumulation rates are often too low, as in the case of the abyssal plains of the SW Iberian Margin [e.g., *Lebreiro et al.*, 1997]. To overcome this difficulty, we correlate the age model obtained for the high-resolution core MC1, located in a shallower area (2173 m depth), with the ^{210}Pb profiles obtained in deeper areas (over 4000 m depth), such as the Infante D. Henrique Basin, and the Tagus and Horseshoe Abyssal Plains.

3.1. Identifying and Dating Turbidite Layers in Core MC1

[10] Core MC1 was characterized by dark yellowish-brown mud for the first 13 cm. A slight oxide layer was identified at 5 cm and laminated sedimentation was observed between 5 and 7 cm. Between 7 and 10 cm, two 1 cm-thick oxide layers with dusky yellowish-brown color were observed (Figure 2a). Thin (1 mm) dark brown bands were also recognized between 10 and 13 cm, attributed to precipitated manganese oxides. From 13 cm to the bottom, the core was characterized by light olive gray compacted mud (Figure 2a). Water content ranged from 60% at the top of the core to 46% at 16 cm depth, although an anomalous peak (58%) was observed at 4–4.5 cm depth (Figure 2b). Hemipelagic sediment was composed of clay (66–68%), silt (29–33%) and sand (1–1.8%). A slight decrease in the clay content (63%) and an increase in the silt fraction (35%) allowed us to identify three detrital layers in the intervals 3–5.5 cm, 7.5–10.5 cm and from 14.5 cm to the bottom (Figure 2c). The location of the MC1 site close to the hilltop of the Marques de Pombal Fault block suggests that these layers are detrital fine perturbations of the hemipelagic sedimentary record.

[11] The bulk mineral composition of MC1 sediments also shows evidence of lithological changes along the core.

The sediments are mainly composed of clay minerals (40–65%), calcite (15–30%) and quartz (10–20%), with lower contents of feldspar (<5%) and dolomite (<5%). The coarse fraction (>50 μm) is composed of calcite (35–65%), quartz (25–45%), feldspars (5–20%) and dolomite (<10%). In core intervals 3–5.5 cm, 7.5–10.5 cm, and 14.5 cm to core bottom, abundance of quartz and feldspar increased up to 45% and 20%, respectively, and calcite decreased down to 35% in the coarse fraction, suggesting terrigenous sediment provenance. Si and K contents also increased in these segments (Figure 2d). These detrital intervals are interpreted as turbidite layers, and hereafter will be referred to as T1, T2 and T3 events (Figure 2).

[12] ^{210}Pb, ^{226}Ra and ^{137}Cs activity profiles of core MC1 are shown in Figure 2. The maximum ^{210}Pb concentration is observed at the top of the core and decreases down to 12 cm depth. The $^{210}Pb_{excess}$ concentration profile does not show the exponential curve expected from radioactive decay due to the presence of the T1 and T2 intervals, where ^{210}Pb activity remains roughly constant and where ^{226}Ra concentrations increase. Variations in the ^{226}Ra concentration are a good indicator of changes in sediment composition in agreement with the geochemical results described above, and allows interpretation of the $^{210}Pb_{excess}$ profile as influenced by rapid sedimentation (turbidites) rather than bioturbation [e.g., *Arnaud et al.*, 2002; *Huh et al.*, 2004, 2006].

[13] In order to determine the age of event T1 (3 to 5.5 cm), sediment accumulation rate (SAR) was estimated for the upper 3 cm using the CF:CS model. The slope of the $\log(^{210}Pb_{excess})$ vs. accumulated mass profile ($R^2 = 0.998$) was used to calculate a SAR of 38 ± 3 mg·cm^{-2}·yr^{-1} (81 ± 7 cm·kyr^{-1}). Therefore, the T1 event would have occurred in 1971 ± 3. Using the same approach, event T2 (7.5 to 10.5 cm) corresponds to 1908 ± 8. Event T3 (14.5 cm to core end) is beyond the limit of the ^{210}Pb method (ca. 1850).

[14] ^{137}Cs is present in the upper 5.5 cm, showing a decreasing concentration from the top with a subsurface maximum at 1.75 cm. The CF:CS model predictions for the depths at which the Chernobyl maximum and the ^{137}Cs onset should be apparent (1.3 cm and 5.75 cm, respectively) agree reasonably well with the ^{137}Cs profile. The 1963 peak should be found between sections 3.50 and 5 cm but it is masked by the T1 turbidite event.

3.2. Linking Turbidites and Earthquake Events in the Marques de Pombal Fault Area

[15] A number of mechanisms such as storm wave loading, hyperpycnal flows, sediment overload, earthquakes, gas hydrate destabilization, etc., have been suggested to account for turbidite triggering [e.g., *Goldfinger et al.*, 2003]. However, in the case of the SW Iberian Margin, earthquakes are the most likely explanation for synchronous, widely-spaced distribution of turbidites during the Holocene period, when sea level was relatively stable [e.g., *Lebreiro et al.*, 1997; *Gràcia et al.*, 2003b; *Vizcaino et al.*, 2006].

[16] The largest seismic events in Western Europe occurred in the SW Iberian Margin [e.g., *Martínez-Solares and López Arroyo*, 2004; *Mezcua et al.*, 2004]. This margin corresponds to the most seismically active and hazardous region in the Iberian Peninsula and it is considered to have a high seismic hazard, between 2.4 and 4.0 m·s^{-2} mean peak ground acceleration with 10% probability of exceedance in 50 years (return period of 475 years) [*Peláez and López Casado*, 2002]. The most catastrophic event was the Lisbon Earthquake (1st of November 1755), with an estimated moment magnitude (Mw) of 8.5–8.7 [e.g., *Johnston*, 1996; *Baptista et al.*, 1998]. This earthquake, which destroyed Lisbon, was accompanied by tsunamis that demolished the coastline along the Gulf of Cádiz and North Atlantic, causing thousands of casualties. Other high-magnitude (Mw > 6) historical and instrumental earthquakes that occurred in the SW Iberian Margin after the 1755 event are located in Figure 1. Coeval with the Lisbon earthquake, a turbidite has been identified in the Horseshoe Abyssal Plain dated by AMS ^{14}C [*Thomson and Weaver*, 1994; *Lebreiro et al.*, 1997].

[17] As regards the turbidite layers identified in core MC1, the ^{210}Pb age of the near-surface event T1 corresponds to 1971 ± 3 yr. An examination of the catalog of large earthquakes in the SW Iberian Margin shows that there is a good temporal correlation with the 28 February 1969 earthquake of Mw 8.0. The epicenter of this earthquake was located in the northeastern part of the Horseshoe Abyssal Plain (Figure 1), about 135 km south of the location where core MC1 was collected. Although the effect of the earthquakes that occurred in 1960 and 1964 could be found in T1, the epicenters were too far away from the sampling site to alter the sediment record. Moreover, it is not known whether these earthquakes triggered any turbidite currents. The age of event T2 corresponds to 1908 ± 8 yr, which fits reasonably well with the 23 April 1909 Benavente earthquake of Mw 6.0 [e.g., *Stich et al.*, 2005b]. The epicenter of this earthquake was located near the Portuguese town of Benavente, about 235 km north of the MC1 site.

3.3. Regional Correlation of Recent Turbidite Events: Paleoseismic Signature

[18] Water content and ^{210}Pb activity profiles of all cores collected in the Tagus and Horseshoe Abyssal Plains and the Infante Don Henrique Basin are depicted in Figure 3. Water content does not decrease uniformly with depth, but shows anomalous peaks denoting the presence of turbidite layers. Moreover, in most cases these anomalies are coincident with intervals where ^{210}Pb concentrations show roughly constant activities, a pattern that can be attributed to turbidite events [e.g., *Huh et al.*, 2004]. Mass accumulation rates are variable among all the six cores (Table 1). They were calculated using the CF:CS model, assuming no deep mixing. Core MC1, located in the shallowest area, has the highest accumulation rate (81 ± 7 cm·kyr^{-1}). Core SW37 has the second highest SAR (55 ± 12 cm·kyr^{-1}), probably because it is located at the base of the Marques de Pombal escarpment, a source of mass transport deposits. The lowest accumulation rates are estimated for cores 9089 and 9099 from the Horseshoe Abyssal Plain (21 ± 1 and 14 ± 2 cm·kyr^{-1}, respectively) (Table 1).

[19] Despite the differences in accumulated mass and accumulation rates, the ^{210}Pb profile patterns of all cores are similar to those of core MC1 (Figures 2 and 3). We observe a near-surface ^{210}Pb disturbed interval corresponding to a turbidite layer (T1) which would correspond to the 1969 AD Horseshoe Earthquake, whose

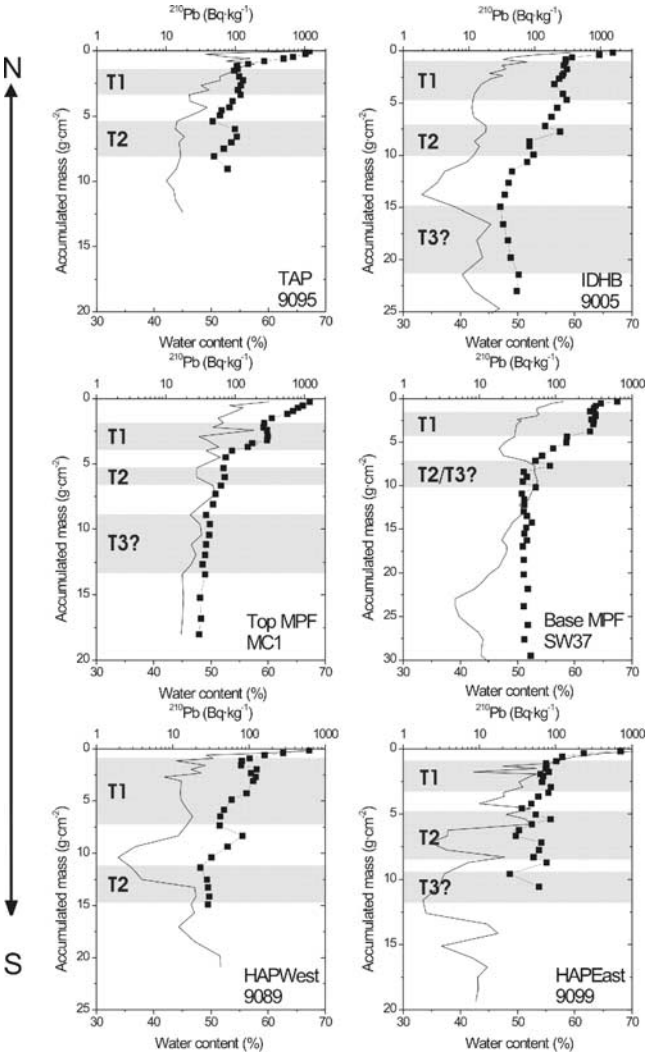

Figure 3. ^{210}Pb profiles in sediment cores. From north to south: Cores 9095, 9005, MC1, SW37, 9089 and 9099. Grey rectangles correspond to turbidite events.

epicentre is located in the abyssal plain. Below the T1 event, two older discontinuities of the expected ^{210}Pb exponential concentration profiles are observed (T2 and T3; Figure 3). The extremely low accumulation rates of the deep cores do not allow us to establish a detailed ^{210}Pb chronology. However, according to the ^{210}Pb profile pattern of core MC1, the turbidite events identified as T2 and T3 would correspond to the 1909 AD Benavente earthquake and to an age older than 1900 AD, most probably associated with the 1858 AD Setubal Earthquake, respectively.

[20] Turbidite paleoseismology has been successfully carried out in active subduction margins, such as Cascadia [e.g., *Goldfinger et al.*, 2003] and Taiwan [*Huh et al.*, 2004, 2006]. In the case of the SW Iberian Margin, the good correlation between turbidites and historical and instrumental seismic events observed for core MC1, and for the five cores collected in adjacent basins and abyssal plains suggests that the turbidite record can also be used as a paleoseismic indicator in a low-convergence rate margin. Thus, turbidite paleoseismology constitutes a valuable tool for earthquake and tsunami hazard assessment in SW Iberia.

[21] **Acknowledgments.** This work was supported by the MCYT Acción Especial HITS (REN2000-2150-E), the Spanish Project IMPULS (REN2003-05996MAR) and the ESF-EUROMARGINS SWIM project (01-LEG-EMA09F and REN2002-11234E-MAR). We thank the captain, crew, scientific and technical staff on board the R/V Hespérides (HITS cruise, PI: E. Gràcia), R/V Sonne (GAP cruise, PI: A. Kopf) and R/V Urania (SWIM-04 cruise, PI: N. Zitellini) for their collaboration. The IAEA wishes to thank the Government of the Principality of Monaco for supporting the Marine Environment Laboratories. We wish to thank the editor and the anonymous reviewers whose constructive criticism enabled us to improve our original manuscript.

References

Adams, J. (1990), Paleoseismicity of the Cascadia subduction zone: Evidence from turbidites off the Oregon-Washington margin, *Tectonics*, *9*, 569–583.

Argus, D. F., R. G. Gordon, C. DeMets, and S. Stein (1989), Closure of the Africa–Eurasia–North America plate motion circuit and tectonics of the Gloria Fault, *J. Geophys. Res.*, *94*, 5585–5602.

Arnaud, F., V. Lignier, M. Revel, M. Desmet, C. Beck, M. Pourchet, F. Charlet, A. Trentesaux, and N. Tribovillard (2002), Flood and earthquake disturbance of ^{210}Pb geochronology (Lake Anterne, NW Alps), *Terra Nova*, *14*, 225–232.

Baptista, M. A., P. M. A. Miranda, J. M. Miranda, and L. Mendes Victor (1998), Constraints of the source of the 1755 Lisbon tsunami inferred from numerical modelling of historical data on the source of the 1755 Lisbon tsunami, *J. Geodyn.*, *259*(2), 159–174.

Buforn, E., C. Sanz de Galdeano, and A. Udias (1995), Seismotectonics of the Ibero-Maghrebian region, *Tectonophysics*, *248*, 247–261.

Buforn, E., M. Beezzeghoud, A. Udias, and C. Pro (2004), Seismic sources on the Iberia-Africa plate boundary and their tectonic implications, *Pure Appl. Geophys.*, *161*, 623–646.

DeMets, C., R. G. Gordon, D. F. Argus, and S. Stein (1990), Current plate motions, *Geophys J. Int.*, *28*, 2121–2124.

Fukao, Y. (1973), Thrust faulting at a lithospheric plate boundary: The Portugal earthquake of 1969, *Earth Planet. Sci. Lett.*, *18*, 205–216.

Goldfinger, C., C. H. Nelson, J. E. Johnson, and Shipboard Scientific Party (2003), Holocene earthquake records from the Cascadia subduction zone and northern San Andreas Fault based on precise dating of offshore turbidites, *Annu. Rev. Earth Planet. Sci.*, *31*, 555–577.

Goldfinger, C., A. Morey, and H. Nelson (2006), Deep-water turbidites as Holocene earthquake proxies along the northern San Andreas Fault system, *Seismol. Res. Lett.*, *77*, 195–196.

Grimison, N. L., and W. P. Chen (1986), The Azores-Gibraltar plate boundary: Focal mechanisms, depths of earthquakes and their tectonic implications, *J. Geophys. Res.*, *91*, 2029–2047.

Gràcia, E., J. J. Dañobeitia, J. Vergés, and PARSIFAL team (2003a), Mapping active faults offshore Portugal (36°N–38°N): Implications for seismic hazard assessment along the southwest Iberian margin, *Geology*, *31*, 83–86.

Gràcia, E., J. Dañobeitia, J. Vergés, R. Bartolomé, and D. Córdoba (2003b), Crustal architecture and tectonic evolution of the Gulf of Cadiz (SW Iberian margin) at the convergence of the Eurasian and African plates, *Tectonics*, *22*(4), 1033, doi:10.1029/2001TC901045.

Huh, C.-A., C.-C. Su, W.-T. Liang, and C.-Y. Ling (2004), Linkages between turbidites in the southern Okinawa Trough and submarine earthquakes, *Geophys. Res. Lett.*, *31*, L12304, doi:10.1029/2004GL019731.

Huh, C. A., C. C. Su, C. H. Wang, S. Y. Lee, and I. T. Lin (2006), Sedimentation in the Southern Okinawa Trough—Rates, turbidites and a sediment budget, *Mar. Geol.*, *231*, 129–139.

Krishnaswami, S., D. Lal, J. M. Martin, and M. Meybecket (1971), Geochronology of lake sediments, *Earth Planet. Sci. Lett.*, *11*, 407–414.

Johnston, A. (1996), Seismic moment assessment of earthquakes in stable continental regions—III. New Madrid, 1811–1812, Charleston 1886 and Lisbon 1755, *Geophys. J. Int.*, *126*, 314–344.

Lebreiro, S. M., I. N. McCave, and P. P. E. Weaver (1997), Late Quaternary turbidite emplacement on the Horseshoe Abyssal Plain (Iberian margin), *J. Sediment. Res.*, *67*(5), 856–870.

López Arroyo, A., and A. Udías (1972), Aftershocks sequence and focal parameters of the Feb. 28, 1969 earthquake of the Azores-Gibraltar fracture zone, *Bull. Seismol. Soc. Am.*, *62*, 699–719.

Martínez-Solares, J. M. (2003), Historical seismicity of the Iberian Peninsula, *Fis. Tierra*, *15*, 13–28.

Martínez-Solares, J. M., and A. López Arroyo (2004), The great historical 1755 earthquake: Effects and damage in Spain, *J. Seismol.*, *8*, 275–294.

Masqué, P., J. Fabres, M. Canals, J. A. Sanchez-Cabeza, A. Sanchez-Vidal, I. Cacho, A. M. Calafat, and J. M. Bruach (2003), Accumulation rates of major constituents of hemipelagic sediments in the deep Alboran Sea: A centennial perspective of sedimentary dynamics, *Mar. Geol.*, *193*, 207–233.

Mezcua, J., J. Rueda, and R. M. Blanco (2004), Reevaluation of historic earthquakes in Spain, *Seismol. Res. Lett.*, *75*, 75–81.

Nittrouer, C. A., R. W. Sternberg, R. Carpenter, and J. T. Bennett (1970), The use of Pb-210 geochronology as a sedimentological tool: Application to the Washington continental shelf, *Mar. Geol.*, *31*, 297–316.

Peláez, J. A., and C. López Casado (2002), Seismic hazard estimate at the Iberian Peninsula, *Pure Appl. Geophys.*, *159*, 2699–2713.

Robbins, J. A., and D. N. Edgington (1975), Determination of recent sedimentation rates in Lake Michigan using Pb-210 and Cs-137, *Geochim. Cosmochim. Acta.*, *39*, 285–304.

Sanchez-Cabeza, J. A., P. Masqué, and I. Ani-Ragolta (1998), ^{210}Pb and ^{210}Po analysis in sediments and soils by microwave acid digestion, *J. Radioanal. Nucl. Chem.*, *227*, 19–22.

Sartori, R., L. Torelli, N. Zitellini, D. Peis, and E. Lodolo (1994), Eastern segment of the Azores-Gibraltar line (central-eastern Atlantic): An oceanic plate boundary with diffuse compressional deformation, *Geology*, *22*, 555–558.

Stich, D., F. de L. Mancilla, and J. Morales (2005a), Crust-mantle coupling in the Gulf of Cadiz (SW-Iberia), *Geophys. Res. Lett.*, *32*, L13306, doi:10.1029/2005GL023098.

Stich, D., J. Batlló, R. Macià, P. Teves-Costa, and J. Morales (2005b), Moment tensor inversion with single-component historical seismograms: The 1909 Benavente (Portugal) and Lambesc (France) earthquakes, *Geophys. J. Int.*, *162*, 850–858.

Terrinha, P., et al. (2003), Tsunamigenic-seismogenic structures, neotectonics, sedimentary processes and slope instability on the southwest Portuguese margin, *Mar. Geol.*, *195*, 55–73.

Thomson, J., and P. P. E. Weaver (1994), An AMS radiocarbon method to determine the emplacement time of recent deep-sea turbidites, *Sediment. Geol.*, *89*, 1–7.

Vizcaino, A., E. Gràcia, R. Pallàs, J. Garcia-Orellana, C. Escutia, D. Casas, V. Willmott, S. Diez, A. Asioli, and J. J. Dañobeitia (2006), Sedimentology, physical properties and ages of mass-transport deposits associated to the Marquês de Pombal Fault, southwest Portuguese margin, *Norw. J. Geol.*, *86*, 173–182.

Zitellini, N., L. Mendes, D. Córdoba, J. J. Dañobeitia, R. Nicolich, G. Pellis, A. Ribeiro, R. Sartori, and L. Torelli (2001), Source of the 1755 Lisbon earthquake and tsunami investigated, *Eos Trans. AGU*, *82*(26), 285–291.

Zitellini, N., M. Rovere, P. Terrinha, F. Chierici, L. Matias, and BIGSETS team (2004), Neogene through Quaternary tectonic reactivation of SW Iberian passive margin, *Pure Appl. Geophys.*, *161*, 565–587.

J. Garcia-Orellana, P. Masqué, C. Olid, and J.-A. Sanchez-Cabeza, Departament de Física, Universitat Autònoma de Barcelona, E-08193 Bellaterra, Spain.

J. Dañobeitia, E. Gràcia, E. Piñero, and A. Vizcaino, Unitat de Tecnologia Marina, CSIC, CMIMA, E-08003 Barcelona, Spain.

F. Martínez-Ruiz, Instituto Andaluz de Ciencias de la Tierra, CSIC, Facultad de Ciencias, Universidad de Granada, Campus Fuentenueva, E-18002 Granada, Spain.